

Transcript Profiling of Non-Target-Site Imidazolinone Resistance in Imisun Sunflower

M. Gil, A. C. Ochogavía, T. Vega,* S. A. Felitti, and G. Nestares

ABSTRACT

Imidazolinone resistance found in a wild sunflower (*Helianthus annuus* L.) population was successfully transferred to a cultivated inbred line developing 'Imisun' sunflowers. Genetic regulation of this trait has been reported to involve two genes: *Imr1*, an allelic variant of *ahas1* locus that codes for acetohydroxyacid synthase catalytic subunit, and the modifier *Imr2*, whose identity remains unknown, but it could be related to non-target-site resistance such as xenobiotic metabolism. The aim of the present study was to characterize the gene expression of resistant and susceptible sunflower lines in response to imazethapyr herbicide by complementary DNA amplified fragment-length polymorphism (cDNA-AFLP). Three assays were performed to determine (i) optimal herbicide treatment concentration, (ii) duration of herbicide treatment, and (iii) in vitro acetohydroxyacid synthase activity to assess enzyme inhibition levels. An important number of genes related to metabolism of xenobiotics and stress was found: cytochrome P450 monooxygenases, UDP-glucuronosyl/UDP-glucosyltransferases, glycosyltransferases, and ATP-binding cassette transporters, among others. These results suggest that non-target-site resistance mechanisms may contribute to herbicide resistance in Imisun sunflower and could be related to the modifier gene *Imr2*. Using cDNA-AFLP, we were able to detect candidate detoxification-related genes potentially involved in imidazolinone resistance in sunflower.

Instituto de Investigaciones en Ciencias Agrarias de Rosario (IICAR, UNR, CONICET), Parque Villarino, S2125ZAA Zavalla, Argentina. Received 1 Feb. 2018. Accepted 14 Jun 2018. *Corresponding author (vega@iicar-conicet.gob.ar). Assigned to Associate Editor Yiqun Weng.

Abbreviations: ABC, ATP-binding cassette; AHAS, acetohydroxyacid synthase; BLAST, Basic Local Alignment Search Tool; cDNA, complementary DNA; cDNA-AFLP, complementary DNA amplified fragment length polymorphism; Cq, quantification cycle; *E*, comparative quantitation; *E* value, measure of the similarity of sequences; EST, expressed sequence tags; GST, glutathione *S*-transferase; NE, normalized expression value; NTSR, non-target-site resistance; PCR, polymerase chain reaction; P450, cytochrome P450 monooxygenase; PVPP, polyvinylpyrrolidone; qRT-PCR, quantitative real-time polymerase chain reaction; TDF, transcript-derived fragment.

A WILD SUNFLOWER (*Helianthus annuus* L.) population (PUR *H. annuus*) resistant to imidazolinones was collected in Kansas (Al-Khatib et al., 1998), and this resistance trait has been introgressed into sunflower elite inbred lines by conventional breeding (Miller and Al-Khatib, 2002; Sala et al., 2012). The developed resistant cultivars, named 'Imisun' sunflowers, were first commercialized as Clearfield sunflowers in 2003 and became a valuable tool for weed management in this species (Tan et al., 2005).

According to Bruniard and Miller (2001), the inheritance patterns of imidazolinone resistance in Imisun sunflower are determined by a digenic model that assumes expression of two resistance genes on both parents to achieve complete resistance in the hybrids *Imr1* and *Imr2*. The major semidominant gene *Imr1* is an allelic variant of the *ahas1* locus that codes for the acetohydroxyacid synthase (AHAS) catalytic subunit, which is the target of imidazolinones (Kolkman et al., 2004). The identity of the modifier gene *Imr2* remains unknown, but it could be related to metabolism of xenobiotics (Breccia et al., 2017). Therefore, resistance in Imisun sunflower appears as a combination of both

Published in Crop Sci. 58:1–11 (2018).
doi: 10.2135/cropsci2018.01.0074

© Crop Science Society of America | 5585 Guilford Rd., Madison, WI 53711 USA
All rights reserved.

target-site and non-target-site resistance (NTSR) mechanisms (Sala et al., 2012).

Target-site mechanisms involve changes in the herbicide binding site of the target enzyme or an increased expression or intrinsic activity of the target protein (Délye et al., 2015). In contrast, NTSR mechanisms consist of a reduction in herbicide penetration and translocation, an enhanced herbicide degradation (metabolic resistance), and/or a protection against the collateral damage of herbicide action (Délye, 2012). Although there are cases of NTSR mechanisms under monogenic control (Mithila et al., 2012), most cases involve polygenic control (Busi et al., 2010; Petit et al., 2010) and include constitutive and inducible effectors. Furthermore, NTSR mechanisms comprise a resistance to multiple modes of action and arise from stress response pathways already present in the plant (Délye et al., 2013).

Non-target-site resistance biochemical bases first involve the oxidation of the herbicide molecule. Afterward, the activated xenobiotic is conjugated using thiols or sugars and actively transported into the vacuole or extracellular space, where it is finally degraded (Yuan et al., 2007). Currently, several gene families have been related to these metabolic resistance processes: cytochrome P450 monooxygenases (P450s), glutathione S-transferases (GSTs), glycosyltransferases, and ATP-binding cassette (ABC) transporters, among others (Manabe et al., 2007; Yuan et al., 2007; Délye, 2012). Few studies have described the participation of these gene families in metabolizing herbicides in the *Helianthus* genera, and they were particularly focused on P450s (Didierjean et al., 2002; Kaspar et al., 2011; Breccia et al., 2017) and GSTs (Balabanova et al., 2017).

According to the hypothesis that imidazolinone resistance in Imisun sunflower involves NTSR mechanisms, the aim of this work was to characterize the transcriptome of resistant (Imisun HA 425) and susceptible (HA 89) sunflower lines in response to imazethapyr herbicide by the transcript profiling method of complementary DNA amplified fragment-length polymorphism (cDNA-AFLP). Optimal concentration and duration of imazethapyr treatment for transcriptome analysis were determined. Additionally, in vitro AHAS activity was evaluated to determine AHAS inhibition levels during herbicide treatment.

MATERIALS AND METHODS

Plant Materials and Growth Conditions

Two near-isogenic lines (NILs) of sunflower were used: HA 425 (*Imr1Imr1Imr2Imr2*) and HA 89 (*imr1imr1imr2imr2*). The resistant line HA 425 is a BC₂F₆ maintainer line resulting from the cross HA 89*3 and PUR *H. annuus* (Miller and Al-Khatib, 2002). HA 89 is a traditional inbred line developed and released by the USDA.

Cypsel were germinated in plastic pots (70 cm³) filled with perlite and watered by capillarity with 1.1 g L⁻¹ of Murashige and Skoog's salts (Murashige and Skoog, 1962) while incubated

at 25 ± 2°C with a 16/8 h light/dark photoperiod (100 μmol m⁻²s⁻¹). The herbicide imazethapyr was used as AHAS inhibitor [active ingredient: 5-ethyl-2-(4-isopropyl-4-methyl-5-oxo-2-imidazolin-2-yl)nicotinic acid].

Optimal Concentration of Imazethapyr

The optimal concentration of imazethapyr for transcriptome analysis was determined using a whole-plant bioassay. At this concentration, also known as the discriminating dose, all susceptible plants die while herbicide-resistant plants exhibit 100% survival with no visible damage after 8 d of treatment (Manabe et al., 2007; R4P Network, 2016).

Plants were obtained as described in the section above. The 8-d-old plants were treated with 0, 0.7, 1, 1.8, 3.3 and 6.6 μM imazethapyr. After 7 d of treatment, plants were collected and dissected, and scanned digital images were acquired. Foliar area, foliar length, and leaf color were evaluated using the Tomato Analyzer 3.0 software (Rodríguez et al., 2010). Leaf color was estimated using the hue angle parameter, which corresponds to a chlorosis index quantified by the Tomato Analyzer Color Test (TACT) (Rodríguez et al., 2010). The effects of the treatments were evaluated by measuring foliar dry weight.

The experimental design was a completely randomized block design with three replicates of 10 plants each. Normality and homogeneity of variance assumptions were tested for each variable, and all data were subjected to ANOVA. Means were separated using Tukey's analysis at the $p = 0.05$ significance level (Sokal and Rohlf, 1962). Statistical analyses were conducted using R software (R Development Core Team, 2010).

Time-Course Studies after Imazethapyr Application

To determine the duration of herbicide treatment, time-course studies were performed. Foliar growth inhibition in presence of imazethapyr was evaluated to exclude the interference on the analysis of genes involved in cell division machinery. Eight-day-old plants were treated with 1 μM imazethapyr for 0, 1, 2, 3, and 4 d. Foliar area, foliar length, and leaf color were evaluated and statistical analyses were performed as described in the section above.

In Vitro Acetohydroxyacid Synthase Activity

To determine AHAS inhibition levels, in vitro enzyme activity was evaluated by quantifying AHAS product acetolactate. Eight-day-old plants were treated with 0 and 1 μM imazethapyr, and both leaves from each plant were collected after 12, 18, and 24 h of treatment. After being weighted, leaves were directly frozen in liquid N. One leaf was saved for cDNA-AFLP, and the second one was sampled for AHAS activity assessment. The in vitro assay was conducted according to Breccia et al. (2013). Briefly, leaves were powdered in liquid N and suspended in buffer (5 mL g⁻¹ fresh wt.) containing 50 mM N(2-hydroxyethyl)-piperazine-N9-(2-ethanesulfonic acid, pH 7.5, 200 mM sodium pyruvate, 20 mM MgCl₂, 2 mM thiamine pyrophosphate, and 20 μM flavin adenine dinucleotide. Insoluble polyvinylpolypyrrolidone (PVPP) was added at the ratio of tissue/insoluble PVPP of 6:1. The homogenate was centrifuged at 27,000g for 10 min at 4°C and immediately used for

enzyme activity assays. Crude extract (140 μL) was incubated at 37°C for 60 min, and afterward it was divided in two aliquots of 70 μL . In one of the aliquots, the reaction was stopped by adding 20 μL of 3 M H_2SO_4 and incubated at 60°C for 15 min to turn acetolactate into acetoin. Acetoin-forming enzymes in plant tissues could affect assay performance (Forlani et al., 1999), thus the contribution of acetoin by non-AHAS enzymes was determined in the second aliquot using 2.5 M NaOH to end the reaction instead of H_2SO_4 . Acetoin concentration was evaluated through a modified colorimetric assay (Westerfeld, 1945), developing the color by adding 135 μL of 0.25% (w/v) creatine and 2.5% (w/v) 1-naphthol prepared in 2.5 M NaOH just before use. The samples were vortexed, incubated at 60°C for 15 min, allowed to cool, and centrifuged at 25°C for 10 min (11,000g). Absorbance was determined spectrophotometrically at 530 nm. The activity of AHAS was expressed as absorbance at 530 nm mg^{-1} fresh wt. as a percentage of the control and was calculated as the mean of three independent determinations. Control and herbicide treatment means were compared using Student's *t* test at the $p = 0.05$ significance level. Statistical analyses were conducted using the “agricolae” and “car” packages in R software (R Development Core Team, 2010).

RNA Extraction and Complementary DNA Synthesis

Total RNA was extracted from leaves collected at different times: 12, 18, and 24 h after imazethapyr treatment. The extraction was performed using a PureLink RNA Mini Kit (Life Technologies) according to the manufacturer's instructions, followed by column DNase I treatment to minimize genomic DNA contamination. Integrity of the RNA was evaluated using both 1.5% agarose gel electrophoresis and spectrophotometric measurements of the 260/280-nm (A_{260}/A_{280}) and 260/230-nm (A_{260}/A_{230}) absorption ratios. Biotinylated oligo dT25, Superscript II (Invitrogen) reverse transcriptase, and DNA polymerase I (Invitrogen) were used for double-stranded cDNA synthesis. Complementary DNA was purified using a Nucleospin Extract II kit (Macherey Nagel) according to the manufacturer's protocols.

cDNA AFLP Analysis and Polyacrylamide Gel Electrophoresis

Optimal restriction enzyme combination was chosen after an in silico analysis using the AFLPInSilico program (Rombauts et al., 2003). The number of transcript-derived fragments (TDFs) was quantified after simulating digestions of sunflower expressed sequence tags (ESTs, available at the National Center for Biotechnology Information (NCBI, <http://www.ncbi.nlm.nih.gov/BLAST>)).

We performed cDNA-AFLP and silver-staining protocols as described by Vuylsteke et al. (2007) and Xiao et al. (2009). Complementary DNA was digested by *Cvi*AI and *Mse*I restriction enzymes and then ligated to corresponding double-stranded adapters (Table 1). The preamplification reaction was performed using specific primers (Table 1) and DNA polymerase GoTaq (Promega). The polymerase chain reaction (PCR) was performed under the following conditions: 30 cycles of 30 s at a melting temperature of 94°C, 30 s at an annealing temperature of 55°C,

1 min at an extension temperature of 72°C, and then 10 min at 72°C. Subsequently, the amplicons were used for selective amplification. The PCR conditions were as follows: 42 cycles including 12 touchdown cycles with a 0.7°C cycle⁻¹ reduction of the initial annealing temperature (65°C), then the reaction was maintained at 55°C for 30 cycles. Table 1 shows the primer combinations used for the selective amplification. The amplicons were separated on a 5% (w/v) polyacrylamide gel electrophoresis at 1300 V for 1 h and 40 min, until bromophenol blue reached the bottom. The bands were visualized by silver staining.

Isolation and Sequencing of Transcript-Derived Fragments

Transcript-derived fragments corresponding to differentially expressed transcripts on polyacrylamide gel electrophoresis were cut out using a razor blade and were incubated in 0.5 M ammonium acetate and 1 mM EDTA for 4 h at 37°C with gentle agitation. The fragments were reamplified under the same PCR conditions as the selective amplification. The resulting PCR products were checked on 2% (m/v) agarose gels as described by Sambrook and Russell (2001). Those presenting the correct size and quality were sent to Macrogen for sequencing analysis (Macrogen, Seoul, Korea).

Sequence identity searches were performed using the Basic Local Alignment Search Tool (BLAST) algorithm by comparison with the de novo sunflower transcriptome generated by Badouin et al. (2017), available at www.heliogene.org/HA412.v1.1.bronze.20141015/. To confirm the identities, sequences were also BLASTed against three databases at NCBI corresponding to plants (taxid: 3193): nucleotide collection (nr/nt), ESTs, and nonredundant protein sequences (nr). The TDFs were classified according to the measures of the similarity of sequences (*E* values) generated in the BLAST search. The *E* values $< 1 \times 10^{-10}$ were deemed to indicate significant identity. We performed BLAST alignments against the sunflower genome (<https://www.heliogene.org/HA412.v1.1.bronze.20141015/>) to identify the corresponding chromosome location for each TDF.

Confirmation of cDNA-AFLP Data by qRT-PCR

Three representative TDFs and one reference gene were evaluated. The reference gene was chosen from cDNA-AFLP analysis as a result of its expression stability over all samples. Specific primer sequences for TDFs were designed with Primer3 0.4.0 software (Rozen and Skaletsky, 2000). Primer sequences used to study the expression of selected TDFs are indicated in Table 2.

Reactions were performed on three biological replicates (one of the RNA samples was the same that was used in the cDNA-AFLP analysis) using three technical replicates.

Total RNA was isolated as described above. The RNA was first treated with DNase and then reversely transcribed into cDNA using an ImProm-II Reverse Transcription System (Promega).

Quantitative real-time PCR (qRT-PCR) was run on a Rotor-Gene Q with a high-resolution melting (Qiagen) thermal cycler. The reaction contained 1 \times SYBR Green PCR Master Mix (Mezcla Real, Biodynamics), 10 μM of the forward and reverse gene-specific primers, and 2 μL cDNA (30 ng) for a final volume of 15 μL . No-template controls were also

Table 1. Adapters and primers used in complementary DNA amplified fragment length polymorphism (cDNA-AFLP) analysis.

Restriction enzyme	Name	Oligonucleotide sequence (5' to 3')
CviAll	CviAll_Forward adapter	CTCGTAGACTGCGTACC
	CviAll_Reverse adapter	ATGGTACGCAGTCTAC
	CviAll_preprimer	CTCGTAGACTGCGTACCAT
	CviAll_selprimerA	GACTGCGTACCATGA
	CviAll_selprimerC	GACTGCGTACCATGC
	CviAll_selprimerG	GACTGCGTACCATGG
	CviAll_selprimerT	GACTGCGTACCATGT
MseI	MseI_Forward adapter	GACGATGAGTCCTGAG
	MseI_Reverse adapter	TACTCAGGACTCAT
	MseI_preprimer	GACGATGAGTCCTGAGTAA
	MseI_selprimerA	GATGAGTCCTGAGTAA
	MseI_selprimerC	GATGAGTCCTGAGTAAC
	MseI_selprimerG	GATGAGTCCTGAGTAAG
	MseI_selprimerT	GATGAGTCCTGAGTAAT

Table 2. Primers used for quantitative real-time polymerase chain reaction.

Gene	Name	Oligonucleotide sequence (5' to 3')
ATP-binding cassette (ABC) transporter	75LeftP	CGCCGTGATCTGACTTTAGC
	75RightP	CCGATGCCTCTAATCATTCCG
Glycosyltransferases	62LeftP	CTCTCCAACGAACCTCCTCC
	62RightP	TATTTTGTCCCCGCCCTCT
	71A_1_20LeftP	CCAATGCTGACTATGCCTGAG
	71A_1_20RightP	GAGGGAAACTTCGGAGGGAA
Reference gene	58LeftP	GGTTGATAAGGAGACGATTGAGT
	58RightP	ACCATTAAGCTATCAGTACCTCC

included. Each cycle consisted of denaturation for 15 s at 94°C, annealing for 60 s at 61 or 62°C (depending on the primer pair), and extension for 40 s at 72°C. Specificity of the amplification reactions was assessed by melting curve analyses, which were run at 95°C for 15 s and 60°C for 15 s, followed by an increase in temperature from 60 to 85°C (0.2°C s⁻¹).

The relative expression of the target genes was assessed using comparative quantitation (*E*) and quantification cycle (*C_q*) values calculated by the software Rotor-Gene Q Series software 1.7 (Corbett Life Science, 2008). The normalized expression value (NE) for each gene was calculated based on *E* and *C_q* in comparison with the reference gene according to Simon's formula: $NE = E_{rg}^{C_{qrg}} / E_{TDF}^{C_{qTDF}}$ (Simon, 2003), where the subscript *rg* indicates a *E* or *C_q* value of the reference gene, and the subscript TDF indicates a *E* or *C_q* value of the TDF. Data were tested for statistical significance by Student's *t* test (*p* = 0.05) using the "agricolae" package in R software (R Development Core Team, 2010).

RESULTS

Optimal Concentration of Imazethapyr

The optimal concentration of imazethapyr for this study was determined by a whole-plant bioassay and was evaluated on resistant (HA 425) and susceptible (HA 89) sunflower lines. Foliar area, foliar length, leaf color (hue angle parameter), and foliar dry weight were evaluated after 7 d of imazethapyr treatment at concentrations of 0, 0.7, 1, 1.8, 3.3, and 6.6 μM (Fig. 1). Line HA 425 was resistant to up to 3.3 μM imazethapyr, whereas in HA 89, phytotoxic

symptoms began at 0.7 μM. According to these results, the optimal concentration of imazethapyr was found to be between 0.7 and 3.3 μM. In this way and consistent with previous studies from the present group, the optimal concentration of herbicide was chosen to be 1 μM.

Time-Course Studies after Imazethapyr Application

To choose the duration of herbicide treatment, time-course studies were performed. Foliar area and foliar length were evaluated during 0, 1, 2, 3, and 4 d of 1 μM imazethapyr treatment (Fig. 2). True leaves in resistant HA 425 plants started to expand 2 d after control treatment (0 μM imazethapyr) and 3 d after 1 μM imazethapyr treatment (Fig. 2). No difference was observed between control and imazethapyr-treated resistant plants throughout the duration of the treatment. On the other hand, no difference was observed between control and imazethapyr-treated susceptible HA 89 plants over the first day of treatment. True leaves in susceptible plants started to expand 1 d after control treatment, whereas imazethapyr-treated plants showed no foliar growth at all. Given these data, cDNA-AFLP analysis was performed from foliar tissue of 8-d-old resistant and susceptible plants, treated with 0 or 1 μM imazethapyr for 12, 18, and 24 h.

In Vitro Acetohydroxyacid Synthase Activity

Inhibition of AHAS activity during the duration of herbicide treatment was evaluated in vitro on leaves from

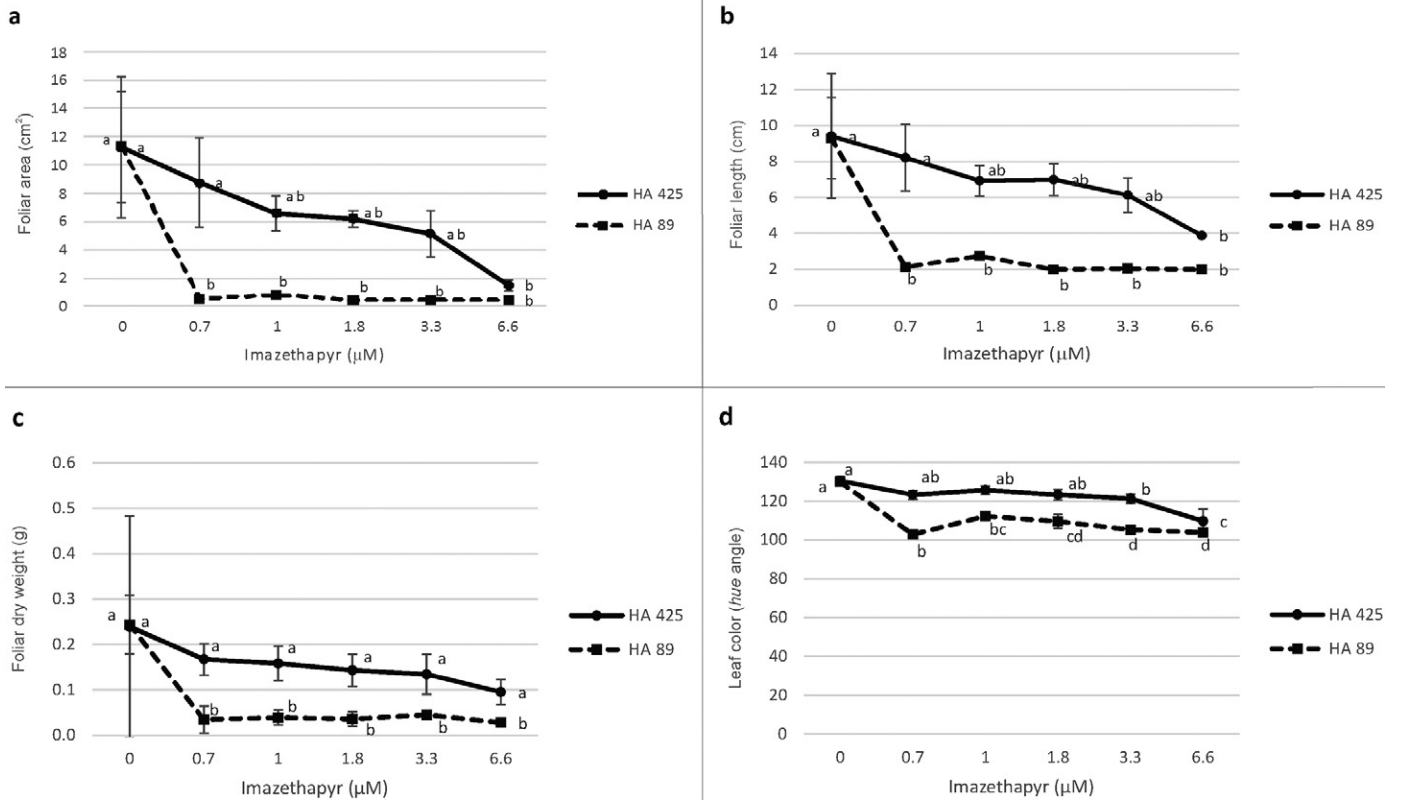


Fig. 1. Optimal concentration of imazethapyr for complementary DNA amplified fragment length polymorphism (cDNA-AFLP) analysis in the resistant (HA 425) and the susceptible (HA 89) sunflower lines. Six different concentrations of imazethapyr were evaluated during 7 d, and mean values were estimated for (a) foliar area (cm²), (b) foliar length (cm), (c) foliar dry weight (g), and (d) leaf color (hue angle). Same letters within a line indicate similar values according to Tukey's test ($p > 0.05$). Vertical bars indicate SEs.

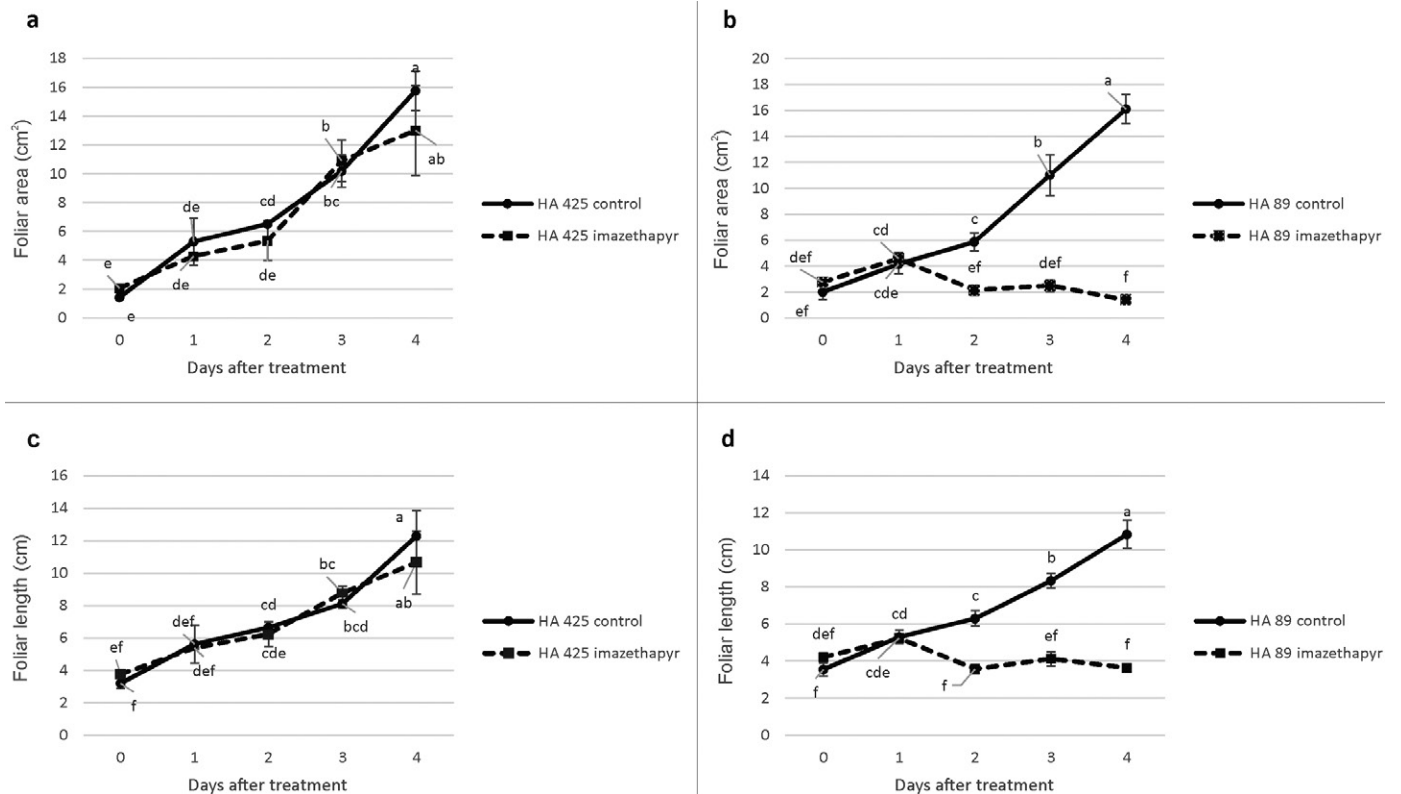


Fig. 2. Effect of imazethapyr on foliar area (cm²) for the (a) resistant (HA 425) and (b) susceptible (HA 89) lines and foliar length (cm) for the (c) resistant (HA 425) and (d) susceptible (HA 89) lines after 4 d of treatment. Vertical bars indicate SEs. Same letters within a line indicate similar values according to Tukey's test ($p > 0.05$).

8-d-old plants after 12, 18, and 24 h of treatment with 1 μM imazethapyr. Activity of AHAS, expressed as absorbance at 530 nm mg^{-1} fresh wt. as a percentage of the control, is shown in Fig. 3.

For the susceptible line, AHAS activity was significantly reduced in imazethapyr-treated with respect to control (0 μM imazethapyr) plants for the three times evaluated. This suggests that imazethapyr molecules are bound to the substrate access channel in the enzyme target site of imidazolinone herbicides. On the other hand, AHAS activity was higher in the resistant line relative to the susceptible line for the three herbicide-treatment times evaluated. In vitro activity was significantly reduced for the resistant line after 18 and 24 h of treatment with 1 μM imazethapyr relative to control plants, whereas no differences were found after 12 h. This agrees with other studies where mutation corresponding to allele *Imr1* confers a moderate resistance to imidazolinone herbicides (Kolkman et al., 2004). The enzyme inhibition is time dependent, involving an initial weak inhibition that becomes progressively stronger with time (Duggleby et al., 2008). These results support the contribution of locus *Imr2* in Imisun sunflower resistance.

cDNA-AFLP Analysis

Transcriptome characterization was conducted using cDNA-AFLP methodology. A total of 16 selective primer combinations were used for this analysis (Table 1). Each combination of primers produced, on average, patterns of ~ 10 fragments per sample, which ranged from 100 to 800 bp. The expression profiles were highly reproducible among biological replicates. A section of a typical cDNA-AFLP polyacrylamide gel profile is shown in Fig. 4.

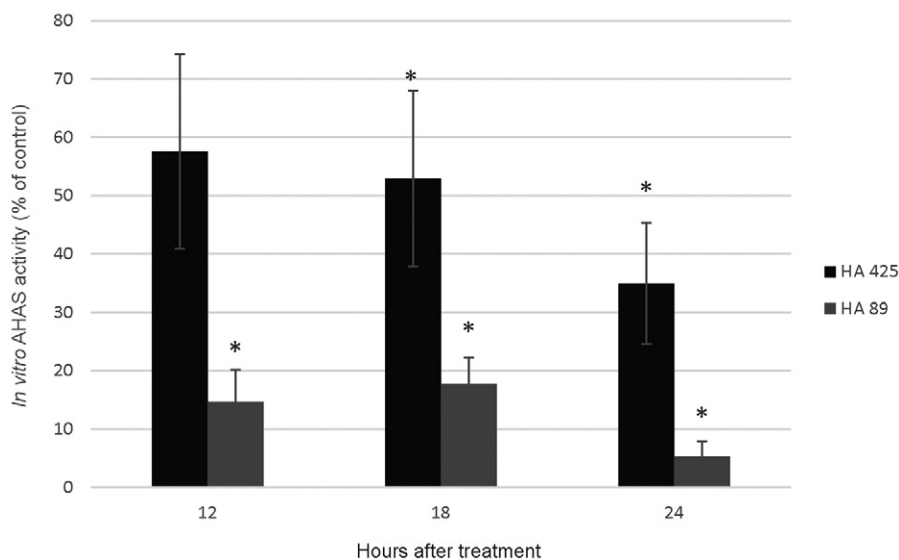


Fig. 3. In vitro acetohydroxyacid synthase (AHAS) activity in resistant (HA 425) and susceptible (HA 89) sunflower lines under 1 μM imazethapyr treatment. Activity was expressed as percentage of the control (0 μM imazethapyr). Vertical bars indicate SEM. Asterisks indicate statistically significant differences from the control (Student's *t* test, $p < 0.05$).

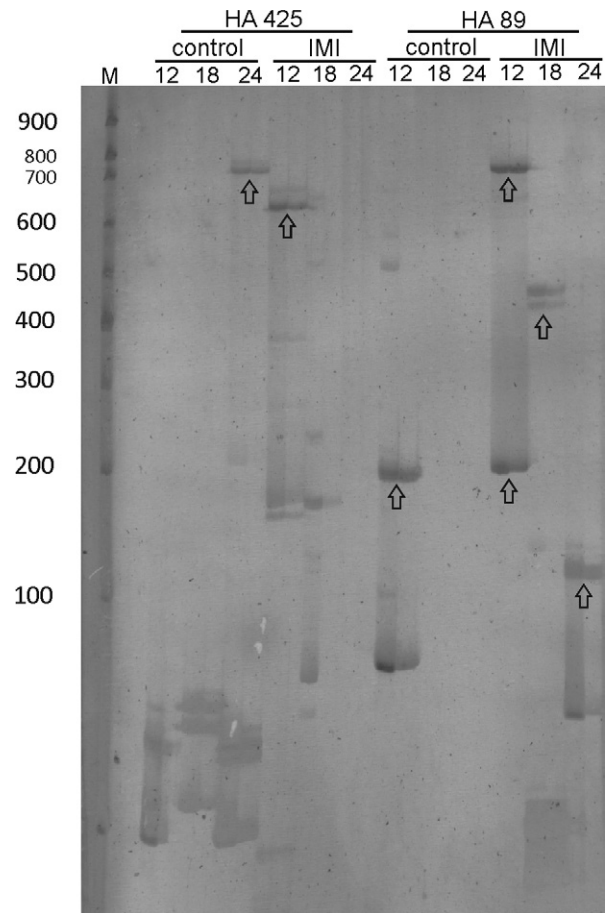


Fig. 4. Section of a complementary DNA amplified fragment length polymorphism (cDNA-AFLP) polyacrylamide gel obtained from selective amplification by using the combination of primers CviAII_selprimerA and MseI_selprimerC. Rows correspond to 12, 18, and 24 h of control and 1 μM imazethapyr (IMI) treatment for the resistant (HA 425) and susceptible (HA 89) sunflower lines together with their technical replicates. M stands for molecular marker. Arrows indicate examples of some of the transcript-derived fragments that were selected for isolation in the analysis.

A total of 1800 TDFs were detected, of which 193 were isolated from gels and reamplified with PCR. These TDFs differed in either presence–absence or intensity along the different samples and therefore were considered to be differentially expressed. The TDFs simultaneously expressed in several samples were also isolated. Fragment sizes were confirmed in agarose gels (data not shown). Forty-nine TDFs were successfully sequenced, presenting a size range of 132 to 533 bp with an average length of 327 bp.

After assignment of putative functions by BLAST similarity search, the 49 TDFs were sorted into 18 functional categories. The largest set of genes corresponded to the functional groups involved in xenobiotic detoxification and drought-induced stress (36%). Four protein families were identified: ABC transporters (14%), glycosyltransferases (10%), cytochrome P450s (2%), and UDP-glucuronosyl/UDP-glycosyltransferases (2%). A minor number of TDFs belonged to particular functions: kinase-related (14%), ribosomal proteins (8%), proteasome and lygases (4% each), N-acetyltransferase activity, aquaporines, Mid1-complementing activity, photosynthesis-related, protein folding, trichome-related, auxine-related, and glyoxylases (2% each). Finally, 16% of the analyzed sequences were included in the unknown category (Fig. 5).

Among the 18 TDFs particularly related to xenobiotic metabolism and drought-induced stress (Table 3):

- Ten were detected in the resistant line HA 425, including four that were upregulated after 12 h of treatment and six that were upregulated after 24 h of treatment. On the other hand, four were found to be upregulated in 0 μ M imazethapyr (control) treatment, three were upregulated in 1 μ M imazethapyr treatment, and three were detected in both treatments.

- Six were detected in the susceptible line HA 89, including four that were upregulated after 12 h of treatment, one after 18 h, and one after 24 h of treatment. Furthermore, two were found to be upregulated in 0 μ M imazethapyr (control) treatment, three were upregulated in 1 μ M imazethapyr treatment, and one was detected in both treatments.
- Two were detected simultaneously in both lines after 24 h of 0 μ M (control) and 1 μ M imazethapyr treatment.

Sequences of the 18 TDFs related to xenobiotic metabolism and drought-induced stress in resistant (HA 425) and susceptible (HA 89) sunflower lines are shown in Supplemental Table S1.

Confirmation of cDNA-AFLP by qRT-PCR

The relative expression of three representative TDFs was analyzed by qRT-PCR: one ABC transporter (75_CviAII_C.ab1512) and two glycosyltransferases (62_CviAII_C.ab1519 and 71A_1_20_CviAII_C.ab1513). They were identified by cDNA-AFLP as all being expressed in resistant sunflower line HA 425 after 12 h of 0 and 1 μ M imazethapyr treatment. Hence, they turned out to be interesting for further characterization. The reference gene was chosen because of its expression stability on cDNA-AFLP analysis, and it was classified as a ribosomal protein (58_CviAII_G.ab1232). Expression levels were evaluated on both resistant (HA 425) and susceptible (HA 89) sunflower lines after 12 h of 0 and 1 μ M imazethapyr treatment (Fig. 6).

The reference gene showed an ideal, uniform behavior between all samples during qRT-PCR analysis (Student's *t* test, $p > 0.05$). The expression profiles were confirmed

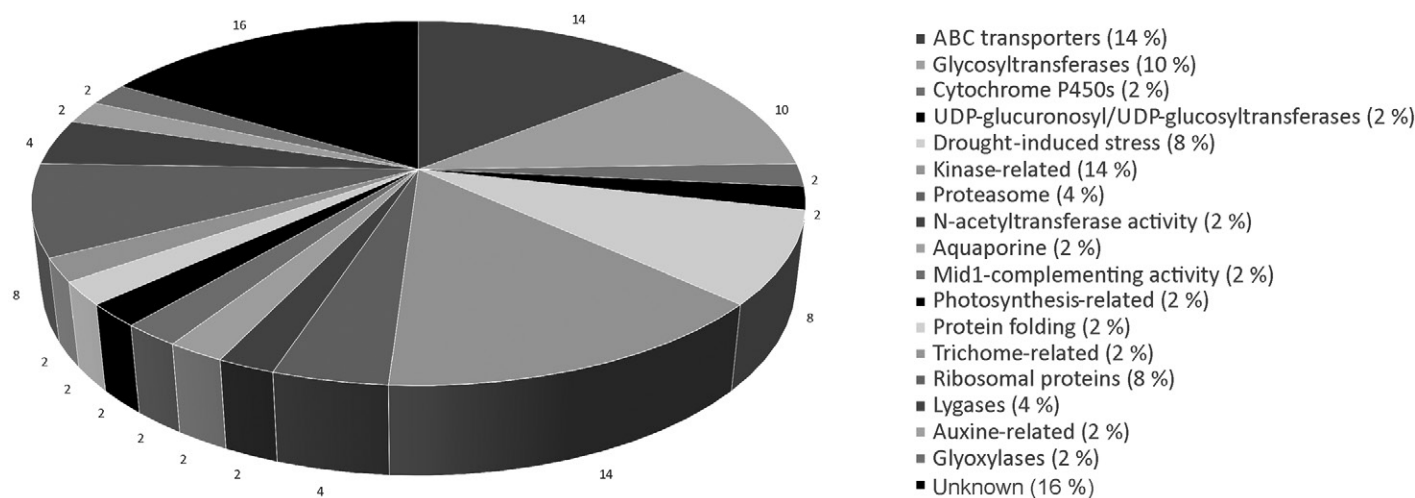


Fig. 5. Functional categories assigned to 49 transcript-derived fragments (TDFs) identified by complementary DNA amplified fragment length polymorphism (cDNA-AFLP) analysis. The transcripts were isolated and sequenced from leaves obtained from resistant (HA 425) and susceptible (HA 89) sunflower lines after 12, 18, and 24 h of 1 μ M imazethapyr. Classes of TDFs were determined using the Basic Local Alignment Search Tool algorithm against the de novo sunflower transcriptome and confirmed blasting against nucleotide collection (nr/nt), expressed sequence tags, and nonredundant protein sequences present in the NCBI database (plant taxid: 3193). The numbers indicate the percentages of TDFs grouped into each functional category.

Table 3. Sequence search results for transcript-derived fragments (TDFs) related to xenobiotic metabolism and drought-induced stress in resistant (HA 425) and susceptible (HA 89) sunflower lines. Total length, imazethapyr treatment, duration of treatment, and chromosome location are indicated for each TDF.

TDF	Sunflower		Imazethapyr		Time after treatment	De novo sunflower transcriptome by local BLAST† ID; name and process			E value‡	Chromosome location	
	Length	line	μM	h		bp					
18_CviAll_C.ab1288	288	HA 425	1	24	288	HA 425	1	24	HaT131113636; IPR013581 Plant PDR ABC transporter associated	3 × 10 ⁻³⁵	Ha11
64_CviAll_C.ab1261	261	HA 425	1	24	261	HA 425	1	24	HaT131030225; IPR003406 Glycosyl transferase, family 14	4 × 10 ⁻⁷³	Ha5
21_CviAll_C.ab1289	289	HA 425	1	12	289	HA 425	1	12	HaT131113636; IPR013581 Plant PDR ABC transporter associated	1 × 10 ⁻³⁸	Ha15
75_CviAll_C.ab1512	512	HA 425	0 and 1	12	512	HA 425	0 and 1	12	HaT131113636; IPR013581 Plant PDR ABC transporter associated	5 × 10 ⁻⁴⁰	Ha4
62_CviAll_C.ab1519	519	HA 425	0 and 1	12	519	HA 425	0 and 1	12	HaT131014865; IPR002495 Glycosyl transferase, family 8	4 × 10 ⁻⁷¹	Ha17
71A_1_20_CviAll_C.ab1513	513	HA 425	0 and 1	12	513	HA 425	0 and 1	12	HaT131014865; IPR002495 Glycosyl transferase, family 8	4 × 10 ⁻⁷¹	Ha9
62_2_CviAll_G.ab1375	375	HA 425	0	24	375	HA 425	0	24	HaT131059899; IPR002213 UDP-glucuronosyl/UDP-glucosyltransferase	4 × 10 ⁻¹⁶⁹	Ha2
48_CviAll_T.ab1301	301	HA 425	0	24	301	HA 425	0	24	HaT131066318; IPR008598 Drought induced 19/RING finger protein 114 AT5G49230.1:symbols:HRB1	3 × 10 ⁻¹⁵	Ha2
49_CviAll_T.ab1306	306	HA 425	0	24	306	HA 425	0	24	HaT131060277; IPR008598 Drought induced 19/RING finger protein 114 AT5G49230.1:symbols:HRB1;AT1G56280.1:symbols:ATD19,DI19	1 × 10 ⁻⁶⁹	Ha13
45_CviAll_T.ab1303	303	HA 425	0	24	303	HA 425	0	24	HaT131008995; IPR008598 Drought induced 19/RING finger protein 114 AT5G49230.1:symbols:HRB1;AT1G56280.1:symbols:ATD19,DI19	9 × 10 ⁻⁴⁸	Ha9
4_CviAll_C.ab1	292	HA 89	1	12	292	HA 89	1	12	HaT131113636; IPR013581 Plant PDR ABC transporter associated	1 × 10 ⁻³⁸	Ha14
17A_CviAll_C.ab1	509	HA 89	1	12	509	HA 89	1	12	HaT131030225; IPR003406 Glycosyl transferase, family 14 Molecular Function: acetylglucosaminyltransferase activity (GO:0008375), Cellular Component: membrane (GO:0016020)	4 × 10 ⁻⁵⁶	Ha9
16A_CviAll_C.ab1	511	HA 89	1	18	511	HA 89	1	18	HaT131014865; IPR002495 Glycosyl transferase, family 8 Molecular Function: transferase activity, transferring glycosyl groups (GO:0016757); AT1G18580.1:symbols:GAUT11; galacturonosyltransferase 11;AT2G20810.1:symbols:GAUT10,LGT4; galacturonosyltransferase 10;AT5G47780.1:symbols:GAUT4	4 × 10 ⁻⁶⁶	Ha10
81_CviAll_C.ab1509	509	HA 89	0 and 1	12	509	HA 89	0 and 1	12	HaT131014865; IPR002495 Glycosyl transferase, family 8 Molecular Function: transferase activity, transferring glycosyl groups (GO:0016757); AT1G18580.1:symbols:GAUT11; galacturonosyltransferase 11;AT2G20810.1:symbols:GAUT10,LGT4; galacturonosyltransferase 10;AT5G47780.1:symbols:GAUT4	5 × 10 ⁻⁷⁰	Ha4
3_CviAll_C.ab1	292	HA 89	0	12	292	HA 89	0	12	HaT131113636; IPR013581 Plant PDR ABC transporter associated	1 × 10 ⁻³⁸	Ha5
5_CviAll_C.ab1295	295	HA 89	0	24	295	HA 89	0	24	HaT131113636; IPR013581 Plant PDR ABC transporter associated	1 × 10 ⁻³⁸	Ha15
59_CviAll_G.ab1169	169	HA 425	0 and 1	24	169	HA 425	0 and 1	24	HaT131138076; IPR001128 Cytochrome P450 Molecular Function: monooxygenase activity (GO:0004497), iron ion binding (GO:0005506), electron carrier activity (GO:0009055), heme binding (GO:0020037); AT3G25180.2:symbols:CYP82G1; cytochrome P450, family 82, subfamily G, polypeptide 1	2 × 10 ⁻⁴⁹	Ha6
44_CviAll_T.ab1492	492	HA 425	0 and 1	24	492	HA 425	0 and 1	24	HaT131066318; IPR008598 Drought induced 19/RING finger protein 114 AT5G49230.1:symbols:HRB1	3 × 10 ⁻⁸⁷	Ha17

† BLAST, Basic Local Alignment Search Tool.

‡ E value, measure of the similarity of sequences.

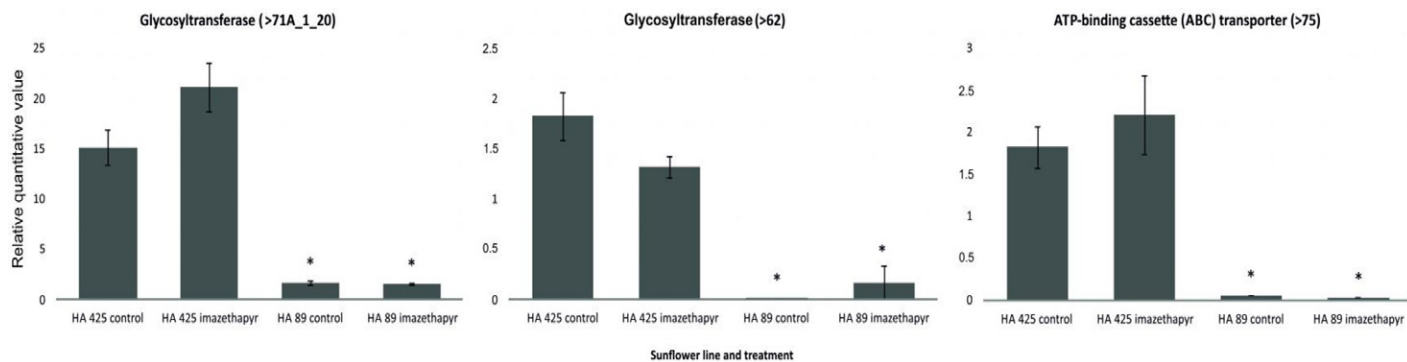


Fig. 6. Relative expression of selected transcript-derived fragments in response to imazethapyr for 12 h in sunflower lines HA 425 and HA 89. Mean values of the relative expression and SEs are shown. Asterisks represent statistically significant differences from the HA_425 control sample analyzed by Student's *t* test ($p < 0.05$).

by qRT-PCR for the three representative TDFs. None of them was found in the susceptible line HA 89 during cDNA-AFLP analysis, and their relative expression levels evaluated by qRT-PCR were negligible in this line.

DISCUSSION

Non-target-site resistance mechanisms generate a reduced number of total herbicide molecules that reach and bind to their target site, thereby preventing xenobiotic deleterious action (Petit et al., 2010). They can affect herbicide penetration, translocation, and accumulation at the target site. Moreover, they can protect the plant against the damages of herbicide action due to an increased expression of genes involved in these metabolic processes (Délye, 2012).

Upregulated genes endowing NTSR may be expected in resistant plants compared with susceptible plants, either before or after herbicide application (constitutive upregulation), or only after herbicide application (herbicide-induced upregulation) (Duhoux and Délye, 2013). In most cases, resistance appears to be constitutive and results from an increase in metabolism that can also be detected in the susceptible genotype (Werck-Reichhart et al., 2000). In resistant genotypes, herbicide-degrading enzymes are generally overproduced or modified, resulting in more efficient herbicide degradation as a result of an increase in specific activity (R4P Network, 2016). This was observed for *Lolium* spp. (Duhoux and Délye, 2013) and *Echinochloa phyllopogon* (Stapf) Koso-Pol. (Iwakami et al., 2014), where P450s-mediated resistance was developed by the overexpression of several P450 genes. Efficient NTSR mechanisms initiate before herbicide damage is irreversible and continue long enough to allow resistant plants to recover and survive (Duhoux et al., 2015).

Complementary DNA amplified fragment length polymorphism is a powerful, robust, and reproducible transcript profiling tool extensively used in diverse species. Here, 49 TDFs identified by cDNA-AFLP analysis were isolated and sequenced from leaves obtained from resistant (HA 425) and susceptible (HA 89) sunflower lines after 12,

18, and 24 h of 1 μ M imazethapyr. In vitro AHAS activity evaluation confirmed that imazethapyr reaches its target site during the times analyzed here and is consistent with previous studies showing the moderate and time-dependent resistance conferred by the allele *Imr1* (Kolkman et al., 2004; Duggleby et al., 2008).

After functional category assignment, 18 sequences were found to be related to xenobiotic metabolism and stress. Among them, 10 sequences were found in the resistant line, six were found in the susceptible line, and two were found in both lines. These results suggest that resistance appears as a consequence of an increase in different metabolism routes that are present in both resistant (HA 425) and susceptible (HA 89) lines. On the other hand, no particular trend was found in relation to the duration of herbicide treatment, and detoxification-related sequences were also detected in control samples. This supports the idea that multiple constitutive NTSR genes participate in imazethapyr resistance in Imisun sunflower.

Sequences related to xenobiotic metabolism were found in this study and corresponded to four families: ABC transporters, glycosyltransferases, P450s, and UDP-glucuronosyl/UDP-glucosyltransferases. Herbicide degradation is a complex process involving the coordinated action of several detoxifying enzymes and regulatory genes like GSTs, glycosyltransferases, ABCs, and P450s, among others (Schäffner et al., 2002; Van Eerd et al., 2003; Manabe et al., 2007; Yuan et al., 2007). In *Arabidopsis thaliana* (L.) Heynh., ABC transporters have been shown to be implicated in detoxification of organic xenobiotics and herbicides (Schulz and Kolukisaoglu, 2006). A structural gene for GST was successfully cloned in rice (*Oryza sativa* L.) and expressed in *Escherichia coli*, which participates in the conjugation of chloroacetanilide herbicides (Cho and Kong, 2005). It was demonstrated that metabolic resistance to diclofop and AHAS inhibitors in *Lolium rigidum* Gaudin was related to the overexpression of P450s, GSTs, and glycosyltransferases (Gaines et al., 2014; Duhoux et al., 2015; Gardin et al., 2015), whereas

the same gene families in addition to ABCs were identified as responsible for resistance to fenoxaprop-P-ethyl in *Beckmannia syzigachne* (Steud.) Fernald (Pan et al., 2016). Particularly in sunflower species, a line with natural resistance to multiple herbicides was found whose resistance was reverted by malathion, an inhibitor of P450s (Kaspar et al., 2011). Moreover, the increased susceptibility to imazapyr after P450 inhibitor treatments suggested that several P450 isozymes were related to herbicide resistance in Imisun cultivars (Breccia et al., 2017). In addition, an involvement of a detoxification system mediated by GSTs was detected in Imisun sunflower hybrids treated with the herbicide imazamox (Balabanova et al., 2017).

Eighteen candidate genes related to metabolic resistance pathways were found in the present transcriptome analysis. Ten of them were particularly expressed in the resistant line, becoming potential detoxification genes involved in imazethapyr resistance in Imisun sunflower. The present study broadens available information about gene expression and imidazolinone resistance mechanisms in sunflower. Novel genetic information was found, becoming an important source for further molecular studies such as isolation and characterization of functional genes. Herbicides are extremely effective tools for weed management, but increasing resistance levels threaten food global production. Gene families potentially involved in herbicide response and NTSR in Imisun sunflower are an important source of variability available for crop breeding.

In conclusion, NTSR mechanisms may contribute to herbicide resistance in Imisun sunflower, and these mechanisms could be related to the modifier locus *Imr2*. This study allowed us to detect constitutively expressed detoxification genes potentially related to imidazolinone resistance in sunflower, encouraging further experimentation to assess the participation of these gene families in herbicide resistance.

Conflict of Interest

The authors declare that there is no conflict of interest.

Supplemental Material Available

Supplemental material for this article is available online.

Acknowledgments

Thanks are due to Dr. Jerry Miller and to Dr. José María Bruniard for kindly gifting seed materials. This work was supported by grants from the Fondo para la Investigación Científica y Tecnológica (PICT 2013-1010) and the Consejo Nacional de Investigaciones Científicas y Técnicas (PUE 0043).

References

Al-Khatib, K., J.R. Baumgartner, D.E. Peterson, and R.S. Currie. 1998. Imazethapyr resistance in common sunflower (*Helianthus annuus*). *Weed Sci.* 46:403–407.

- Badouin, H., J. Gouzy, C. Grassa, F. Murat, S. Staton, L. Cotret, et al. 2017. The sunflower genome provides insights into oil metabolism, flowering and Asterid evolution. *Nature* 546:148–152. doi:10.1038/nature22380
- Balabanova, D., T. Remans, A. Vassilev, A. Cuyppers, and J. Vangronsveld. 2017. Possible involvement of glutathione S-transferases in imazamox detoxification in an imidazolinone-resistant sunflower hybrid. *J. Plant Physiol.* 221:62–65. doi:10.1016/j.jplph.2017.12.008
- Breccia, G., M. Gil, T. Vega, E. Altieri, M. Bulos, L. Picardi, and G. Nestares. 2017. Contribution of non-target-site resistance in imidazolinone-resistant Imisun sunflower. *Bragantia* 76:536–542. doi:10.1590/1678-4499.2016.336
- Breccia, G., T. Vega, S.A. Felitti, L. Picardi, and G. Nestares. 2013. Differential expression of acetohydroxyacid synthase genes in sunflower plantlets and its response to imazapyr herbicide. *Plant Sci.* 208:28–33. doi:10.1016/j.plantsci.2013.03.008
- Bruniard, J.M., and J.F. Miller. 2001. Inheritance of imidazolinone-herbicide resistance in sunflower. *Helia* 24:11–16.
- Busi, R., M.M. Vila-Aiub, and S.B. Powles. 2010. Genetic control of a cytochrome P450 metabolism-based herbicide resistance mechanism in *Lolium rigidum*. *Heredity* 106:817–824. doi:10.1038/hdy.2010.124
- Cho, H.Y., and K.H. Kong. 2005. Molecular cloning, expression, and characterization of a phi-type glutathione S-transferase from *Oryza sativa*. *Pestic. Biochem. Physiol.* 83:29–36. doi:10.1016/j.pestbp.2005.03.005
- Corbett Life Science. 2008. Rotor-Gene Q Series software 1.7. Build 94. Corbett Life Sci., Sydney, NSW.
- Délye, C. 2012. Unravelling the genetic bases of non-target-site-based resistance (NTSR) to herbicides: A major challenge for weed science in the forthcoming decade. *Pest Manag. Sci.* 69:176–187. doi:10.1002/ps.3318
- Délye, C., A. Duhoux, F. Pernin, C.W. Riggins, and P.J. Tranel. 2015. Molecular mechanisms of herbicide resistance. *Weed Sci.* 63:91–115. doi:10.1614/WS-D-13-00096.1
- Délye, C., M. Jasieniuk, and V. Le Corre. 2013. Deciphering the evolution of herbicide resistance in weeds. *Trends Genet.* 29:649–658. doi:10.1016/j.tig.2013.06.001
- Didierjean, L., L. Gondet, R. Perkins, S.C. Lau, H. Schaller, D.P. O’Keefe, and D. Werck-Reichhart. 2002. Engineering herbicide metabolism in tobacco and *Arabidopsis* with CYP76B1, a cytochrome P450 enzyme from Jerusalem artichoke. *Plant Physiol.* 130:179–189. doi:10.1104/pp.005801
- Duggleby, R.G., J.A. Mccourt, and L.W. Guddat. 2008. Structure and mechanism of inhibition of plant acetohydroxyacid synthase. *Plant Physiol. Biochem.* 46:309–324. doi:10.1016/j.plaphy.2007.12.004
- Duhoux, A., S. Carrère, J. Gouzy, L. Bonin, and C. Délye. 2015. RNA-Seq analysis of rye-grass transcriptomic response to an herbicide inhibiting acetolactate-synthase identifies transcripts linked to non-target-site-based resistance. *Plant Mol. Biol.* 87:473–487. doi:10.1007/s11103-015-0292-3
- Duhoux, A., and C. Délye. 2013. Reference genes to study herbicide stress response in *Lolium* sp.: Up-regulation of P450 genes in plants resistant to acetolactate-synthase inhibitors. *PLoS One* 8:e63576. doi:10.1371/journal.pone.0063576
- Forlani, G., M. Mantelli, and E. Nielsen. 1999. Biochemical evidence for multiple acetoin-forming enzymes in cultured plant cells. *Phytochemistry* 50:255–262. doi:10.1016/S0031-9422(98)00550-0

- Gaines, T.A., L. Lorentz, A. Figge, J. Herrmann, F. Maiwald, M.C. Ott, et al. 2014. RNA-Seq transcriptome analysis to identify genes involved in metabolism-based diclofop resistance in *Lolium rigidum*. *Plant J.* 78:865–876. doi:10.1111/tbj.12514
- Gardin, J.A.C., J. Gouzy, S. Carrère, and C. Délye. 2015. ALO-MYbase, a resource to investigate non-target-site-based resistance to herbicides inhibiting acetolactate-synthase (ALS) in the major grass weed *Alopecurus myosuroides* (black-grass). *BMC Genomics* 16:590–612. doi:10.1186/s12864-015-1804-x
- Iwakami, S., A. Uchino, Y. Kataoka, H. Shibaike, H. Watanabe, and T. Inamura. 2014. Cytochrome P450 genes induced by bispyribac-sodium treatment in a multiple-herbicide-resistant biotype of *Echinochloa phyllopogon*. *Pest Manag. Sci.* 70:549–558. doi:10.1002/ps.3572
- Kaspar, M., M. Grondona, A. Leon, and A. Zambelli. 2011. Selection of a sunflower line with multiple herbicide tolerance that is reversed by the P450 inhibitor malathion. *Weed Sci.* 59:232–237. doi:10.1614/WS-D-10-00120.1
- Kolkman, J.M., M.B. Slabaugh, J.M. Bruniard, S. Berry, B.S. Bushman, C. Olungu, et al. 2004. Acetohydroxyacid synthase mutations conferring resistance to imidazolinone or sulfonylurea herbicides in sunflower. *Theor. Appl. Genet.* 109:1147–1159. doi:10.1007/s00122-004-1716-7
- Manabe, Y., N. Tinker, A. Colville, and B. Miki. 2007. CSR1, the sole target of imidazolinone herbicide in *Arabidopsis thaliana*. *Plant Cell Physiol.* 48:1340–1358. doi:10.1093/pcp/pcm105
- Miller, J.F., and K. Al-Khatib. 2002. Registration of imidazolinone herbicide-resistant sunflower maintainer (HA 425) and fertility restorer (RHA 426 and RHA 427) germplasm. *Crop Sci.* 42:988–989. doi:10.2135/cropsci2002.988a
- Mithila, J., M.D. McLean, S. Chen, and J. Christopher Hall. 2012. Development of near-isogenic lines and identification of markers linked to auxinic herbicide resistance in wild mustard (*Sinapis arvensis* L.). *Pest Manag. Sci.* 68:548–556. doi:10.1002/ps.2289
- Murashige, T., and F. Skoog. 1962. A revised medium for rapid growth and bioassays with tobacco tissue cultures. *Physiol. Plant.* 15:473–497. doi:10.1111/j.1399-3054.1962.tb08052.x
- Pan, L., H. Gao, W. Xia, T. Zhang, and L. Dong. 2016. Establishing a herbicide-metabolizing enzyme library in *Beckmannia syzigachne* to identify genes associated with metabolic resistance. *J. Exp. Bot.* 67:1745–1757.
- Petit, C., B. Duhieu, K. Boucansaud, and C. Délye. 2010. Complex genetic control of non-target-site-based resistance to herbicides inhibiting acetyl-coenzyme A carboxylase and acetolactate-synthase in *Alopecurus myosuroides* Huds. *Plant Sci.* 178:501–509. doi:10.1016/j.plantsci.2010.03.007
- R Development Core Team. 2010. R: A language and environment for statistical computing. R Found. Stat. Comput., Vienna.
- R4P Network. 2016. Trends and challenges in pesticide resistance detection. *Trends Plant Sci.* 21:834–853. doi:10.1016/j.tplants.2016.06.006
- Rodríguez, G.R., J.B. Moyseenko, M.D. Robbins, N.H. Morejón, D.M. Francis, and E. van der Knaap. 2010. Tomato Analyzer: A useful software application to collect accurate and detailed morphological and colorimetric data from two-dimensional objects. *J. Vis. Exp.* 37:e1856. doi:10.3791/1856
- Rombauts, S., Y. van de Peer, and P. Rouzé. 2003. AFLP/Silico, simulating AFLP fingerprints. *Bioinformatics* 19:776–777. doi:10.1093/bioinformatics/btg090
- Rozen, S., and H.J. Skaletsky. 2000. Primer3 on the WWW for general users and for biologist programmers. In: S. Krawetz and S. Misener, editors, *Bioinformatics methods and protocols: Methods in molecular biology*. Humana Press, Totowa, NJ. p. 365–386.
- Sala, C.A., M. Bulos, E. Altieri, and M.L. Ramos. 2012. Genetics and breeding of herbicide tolerance in sunflower. *Helia* 35:57–69. doi:10.2298/HEL1257057S
- Sambrook, J., and D.W. Russell. 2001. *Molecular cloning: A laboratory manual*. Cold Spring Harbor Lab. Press, Cold Spring Harbor, NY.
- Schäffner, A., B. Messner, C. Langebartels, and H. Sandermann. 2002. Genes and enzymes for in-plant phytoextraction of air, water and soil. *Acta Biotechnol.* 22:141–151. doi:10.1002/1521-3846(200205)22:1/2<141::AID-ABIO141>3.0.CO;2-7
- Schulz, B., and H.Ü. Kolukisaoglu. 2006. Genomics of plant ABC transporters: The alphabet of photosynthetic life forms or just holes in membranes? *FEBS Lett.* 580:1010–1016.
- Simon, P. 2003. Q-Gen: Processing quantitative real-time RT-PCR data. *Bioinformatics* 19:1439–1440. doi:10.1093/bioinformatics/btg157
- Sokal, R.R., and F.J. Rohlf. 1962. *Biometry: The principles and practices of statistics in biological research*. WH, Freeman & Co., San Francisco.
- Tan, S., R.R. Evans, M.L. Dahmer, B.K. Singh, and D.L. Shaner. 2005. Imidazolinone-tolerant crops: History, current status and future. *Pest Manag. Sci.* 61:246–257. doi:10.1002/ps.993
- Van Eerd, L.L., R.E. Hoagland, R.M. Zablutowicz, and J.C. Hall. 2003. Pesticide metabolism in plants and microorganisms: An overview. *Weed Sci.* 51:472–495.
- Vuylsteke, M., J.D. Peleman, and M.J.T. van Eijk. 2007. AFLP-based transcript profiling (cDNA-AFLP) for genome-wide expression analysis. *Nat. Protoc.* 2:1399–1413.
- Werck-Reichhart, D., A. Hehn, and L. Didierjean. 2000. Cytochromes P450 for engineering herbicide tolerance. *Trends Plant Sci.* 5:116–123. doi:10.1016/S1360-1385(00)01567-3
- Westerfeld, W.W. 1945. A colorimetric determination of blood acetoin. *J. Biol. Chem.* 161:495–502.
- Xiao, X., H. Li, and C. Tang. 2009. A silver-staining cDNA-AFLP protocol suitable for transcript profiling in the latex of *Hevea brasiliensis* (para rubber tree). *Mol. Biotechnol.* 42:91–99. doi:10.1007/s12033-008-9139-3
- Yuan, J.S., P.J. Tranel, and C.N. Stewart. 2007. Non-target-site herbicide resistance: A family business. *Trends Plant Sci.* 12:6–13. doi:10.1016/j.tplants.2006.11.001